Sensors and Actuators A 183 (2012) 22–27

Contents lists available at SciVerse ScienceDirect

Sensors and Actuators A: Physical

journal homepage: www.elsevier.com/locate/sna

Biosensor based on hollow-core metal-cladding waveguide

Pingping Xiao[a,b], Xianping Wang[a,*], Jingjing Sun[a], Honggen Li[a], Meizhen Huang[a], Xianfeng Chen[a], Zhuangqi Cao[a]

[a] Department of Physics, the State Key Laboratory on Fiber Optic Local Area Communication Networks and Advanced Optical Communication Systems, JiaoTong University, Shanghai 200240, China
[b] School of Physics Science and Engineering Technology, Yichun University, Yichun 336000, China

ARTICLE INFO

Article history:
Received 21 November 2011
Received in revised form 30 May 2012
Accepted 30 May 2012
Available online 21 June 2012

Keywords:
Biosensor
Optical waveguide
High sensitivity

ABSTRACT

A new hollow-core metal-cladding waveguide (HCMW) has been proposed in order to design and realize optical biosensor for the direct liquid probing. Two peculiar properties are exhibited with respect to the current evanescent wave sensors. First, the effective index of the HCMW can exist in the region of $0 < N < 1$, which is usually prohibited for the conventional guided modes and the surface plasmon resonance modes. Second, the analyte to be detected does not locate in the evanescent field but in the oscillating field. Glucose solution is utilized to characterize the device performance. According to the reflectivity changes and the signal-to-noise ratio, the new biosensor has been shown to be capable of directly detecting concentration of glucose as low as 0.5 ppm, which corresponds to a high resolution of 1.4×10^{-7} RI units. This new biosensor improves the detection limitation and shortens the analysis time significantly.

1. Introduction

The need for rapid and sensitive detection of microorganisms and their interactions is very important in areas of food safety, medical care, environmental protection, and biological warfare [1–7]. Among various detecting approaches, biosensors based on optical resonant mode are the subject of growing interest due to their peculiar properties, such as relatively high sensitivity, fast response, small dimensions, and high mechanical stability. Techniques reported include surface plasmon resonance (SPR) [8,9], long-range surface plasmon resonance (LRSPR) [10], resonant mirror (RM) [11], leaky mode waveguide (LMW) [12], reverse symmetrical waveguide (RSM) [13] and metal-clad leaky waveguide (MCLW) [14–16]. The common feature of these current sensors is that the analyte to be detected is located in the region where the evanescent wave of the resonant modes propagates. According to the sensitivity analysis, the use of such evanescent wave biosensors is problematic due to the limited sensitivity resulting from several reasons [4]. These include (1) the limited power portion propagating in the sensing region where the analyte is located; (2) refractive index of the analyte must be always less than the effective index of the resonant modes; (3) the short penetration depth of the evanescent field makes the large analytes, such as bacteria, outside the sensing region, resulting in further insufficient sensitivity of the system.

To achieve a high sensitivity, it is essential to get as much of the optical power as possible to propagate in the sensing region. Investigation of the mode power distribution suggests us to design a configuration that contains the sample in the guiding layer of the waveguide, where oscillating wave is located and most of the mode power concentrates. Addressed this issue, a sensor structure based on porous silicon (PS) waveguide [17] is proposed, in which the target material is filled inside the porous silicon where the oscillating field propagates. Theoretical calculations indicate that the PS sensor shows a greater sensitivity than the conventional SPR sensors. However, sensitivity enhancement is also limited due to the limited volume of the analyte locates in the region of oscillating field. Recently, several chemical and biological sensors based on liquid-core waveguides (LCWG) have been proposed to improve the detection efficiency [18]. Unfortunately, this idea is severely blocked by conventional waveguiding, since water-based solvent has a lower index than almost all the solids which acts as the clad layer of the waveguide.

Facing the above challenge in the biosensors, we proposed a hollow-core metal-cladding waveguide (HCMW) structure in which the hollow-core of sub-millimeter scale is surrounded by metal claddings. In this design the use of double metal claddings which exhibit negative dielectric constant implies that the effective index of the guided modes can exist in the region of $0 < N < 1$ [19], which is usually prohibited for the conventional guided modes and the surface plasmon resonance modes [20]. Analyte of interest

* Corresponding author.
E-mail addresses: xpwangphysics@gmail.com (X. Wang), zqcao@sjtu.edu.cn (Z. Cao).

0924-4247/$ – see front matter © 2012 Elsevier B.V. All rights reserved.
http://dx.doi.org/10.1016/j.sna.2012.05.047

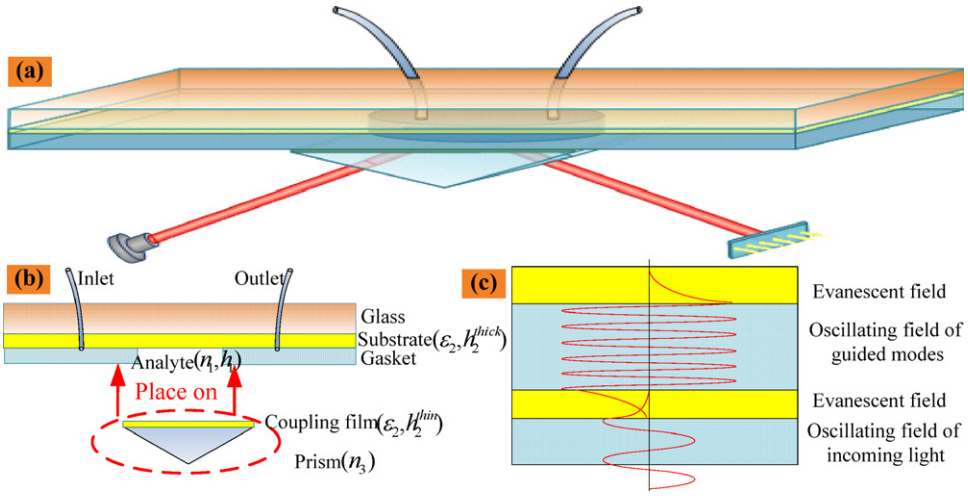

Fig. 1. Schematic diagram of hollow-core metal-cladding waveguide (HCMW): (a) stereogram, (b) plan view, (c) graphical representation of field distribution in HCMW.

contained in the hollow core serves as guiding medium where oscillating wave propagates. Furthermore, in the HCMW structure, the thickness of guiding layer can be expanded to sub-millimeter scale, which makes it easy to inject the aqueous sample into the guiding layer and to excide the sensitive ultrahigh-order modes [21]. It is expected that guiding both light and liquid through the same physical volume maximizes their interaction and should allow for extremely sensitive and rapid sensing. In order to characterize the device performance, a significantly lower concentration of glucose is utilized in our experiment. In the conventional biosensor [22,23], glucose usually is present in relatively high concentrations so that most assays have been developed for a rather high concentration range. Nevertheless, analytical methods for relatively small concentrations of glucose are needed as well, for example when analyzing body fluids that do contain low concentrations (such as tear, sweat and urine). Owing to (1) light power concentrated in the guiding region can enlarge the interaction with the analyte of interest; (2) using of the ultrahigh-order modes with smaller effective index further increases the interaction distances, concentration of glucose as low as 0.5 ppm has been unambiguously identified in our experiment within a several minutes assay. The proposed HCMW sensor exhibits a minimum refractive index variation of $\Delta n = 1.4 \times 10^{-7}$. Aside from higher detection efficiency, the proposed platform offers additional benefits: such as small analyte volume, label-free and real-time detection, and enables environmentally stable, compact, and inexpensive sensing.

2. Hollow-core metal-cladding waveguide

The schematic diagram of hollow-core metal-cladding waveguide (HCMW) in our experiment is illustrated in Fig. 1. Excepting a glass prism with a big vertex angle which serves as a coupling element, HMCW is basically a three-layered optical waveguide, analyte solution confined in hollow core acts as the guided medium, while the two metal films serve as the claddings. For simplicity in sensitivity analysis, we neglect the effects resulting from the limited thickness of the metal film due to the weak coupling [24], dispersion equation of the HCMW can then be written as [21]

$$\kappa_1 h_1 = m\pi + 2\arctan\left|\rho\frac{\alpha_2}{\kappa_1}\right|, \quad (m = 0, 1, 2, \cdots), \tag{1}$$

where $\rho = 1$ for TE modes, while $\rho = \varepsilon_1/\varepsilon_2$ for TM modes. $\varepsilon_1 = n_1^2$ and ε_2 represent dielectric constants of the analyte and the metal films, respectively. h_1 is the thickness of the analyte and m is mode-order number. The vertical propagation constant κ_1 in the guiding medium and the decay coefficient α_2 in the metal claddings are defined by

$$\begin{cases} \kappa_1 = (k_0^2 n_1^2 - \beta^2)^{1/2} \\ \alpha_2 = (\beta^2 - k_0^2 \varepsilon_2)^{1/2} \end{cases}, \tag{2}$$

$k_0 = 2\pi/\lambda$ is the wavenumber with light wavelength λ in free space, and $\beta = k_0 N$ is the transverse propagation constant with the effective index N of the guided modes. For most commonly used noble metals in the visible and near-infrared regions, since the imaginary part of its dielectric constant is much less than its real part, it is often convenient to neglect the imaginary part in the analysis. The dispersive curves of the HCMW are shown in Fig. 2. When the thickness of the guiding medium is extended to sub-millimeter scale (see the dashed line $h_1 = 700\ \mu m$), the waveguide can accommodate thousands of guide modes ($m > 1000$), in our terminology, we denote these modes as ultrahigh-order modes [21]. Since the real part of the dielectric constant of the coupling film (metal) is negative, the allowed range of the effective index of both TE and TM modes of proposed HCMW is $0 < N < n_1$ [20]. It is quite different from the conventional guided modes and the surface plasmon

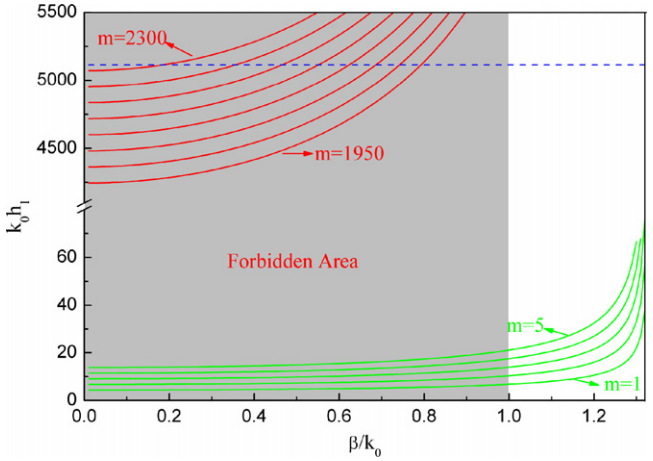

Fig. 2. Dispersive curves of the HCMW with the parameters: $n_1 = 1.330$, $\varepsilon_2 = -10.2$, $\lambda = 632.8$ nm. The blue transverse dashed line denotes $h_1 = 700\ \mu m$, the red and green curves indicate the ultrahigh-order modes and low order modes, respectively. (For interpretation of the references to color in this figure legend, the reader is referred to the web version of this article).

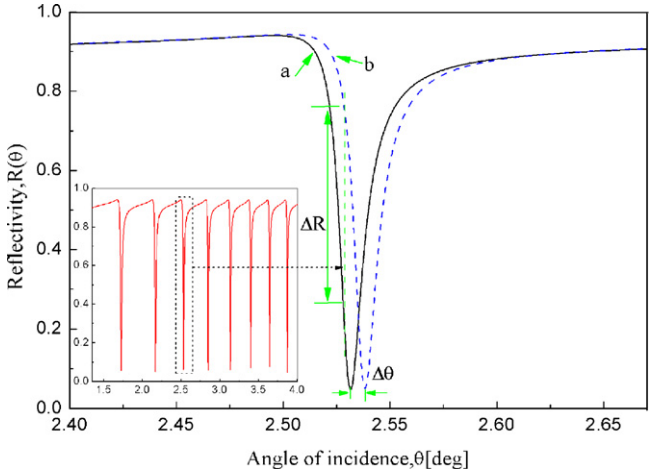

Fig. 3. Change of the reflectivity caused by the resonant angle shift of the incident light. Inset: Simulated ATR curve for ultrahigh-order modes with the following parameters: $n_3 = 1.517$, $h_2^{thin} = 50\,\text{nm}$, $h_2^{thick} = 200\,\text{nm}$, $n_1 = 1.330$, $h_1 = 700\,\mu\text{m}$, $\varepsilon_2 = -10.2 + 1.6i$, $\lambda = 632.8\,\text{nm}$.

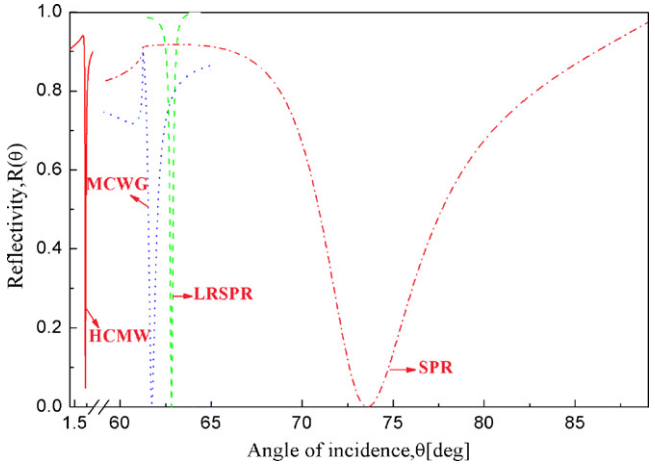

Fig. 4. Theoretical comparison for four optical biosensors: SPR, LRSPR, MCWG, and HCMW. The compositions of the four sensor types are listed in Table 2.

resonance, in which the effective index N must be greater than that of the cover medium, the region of $0 < N < 1$ is absolutely prohibited.

HCMW sensor is operated with the attenuated total reflection scheme in which a polarized laser beam is incident from the prism-side and the reflectance R is measured as a function of the angle of incidence. During the angle scanning, a series of resonance dips with respect to the excitation of the guided modes are then produced a so-called attenuated total reflection (ATR) spectrum. Position of the resonance dip indicates the effective index of the guided mode and is very sensitive to the change of refractive index of the guiding layer. A minute variation in the concentration of the aqueous solution will consequently cause an angular shift of the resonance dip. By monitoring the angular shift of the resonance dip, the change in solution concentration can be measured. The resonance excitation of the guided mode occurs at [21]

$$\beta = k_0 n_3 \sin\theta, \tag{3}$$

where n_3 represents refractive index of the prism, and θ is the angle of incidence. As shown in Fig. 3, if θ is small, ultrahigh-order modes with $N \to 0$ will then be excited under the condition of resonance excitation.

3. Sensitivity analysis

ATR spectrums for one and a small number of the ultrahigh-order modes are shown in Fig. 3. It is shown that the falling edge and the rising edge of a reflection dip exhibit quite favorable linearity. In this case we fix the angle of incidence near the mid point of the falling edge of a reflection dip and monitor changes in the reflectivity ΔR caused by shift of the resonance angle $\Delta\theta$, which is resulted from changes of the analyte concentration. In this intensity interrogation mode [25], the sensitivity can be defined as:

$$S = \frac{\partial R}{\partial n_{guide}} = \left(\frac{\partial R}{\partial \theta}\right)_{\theta=\theta_s} \cdot \left(\frac{\partial \theta}{\partial n_{guide}}\right) = S_1 \cdot S_2. \tag{4}$$

Obviously, S_1 represents the slope of the falling edge at the operation angle θ_s, it is strongly dependent on the full-width-half-maximum (FWHM) of the dip. The narrower of the dip, the bigger of S_1. Theoretical comparisons of the FWHM for HCMW, SPR, LRSPR, and MCLW are demonstrated in Fig. 4. As is shown, the FWHM of the reflectivity curves is broadest in the conventional SPR and gets narrower one by one in the MCWG, LRSPR and HCMW configurations. It is clear that the HCMW sensor relative to the other three types of sensor has a FWHM at least an order of magnitude less.

Meanwhile, S_2 represents the detect efficiency or the sensitivity in angular exploration mode of the HCMW sensor. To be clear, we use n_{guide} as the refractive index of the analyte confined in the hollow core. Without loosing any generality, we neglect the effect of a less important factor $1/(n_3 \cos\theta)$ and consider TE modes only here. After a rather lengthy derivation, S_2 can be expressed as [26]

$$S_2 = \frac{\partial N}{\partial n_{guide}} = \frac{n_{guide}}{N} \cdot \frac{p_{guide}}{P_{total}}, \tag{5}$$

and

$$\frac{p_{guide}}{p_{total}} = \frac{h_1 + 2\alpha_2/(\kappa_1^2 + \alpha_2^2)}{h_1 + 2/\alpha_2}, \tag{6}$$

where p_{guide} represents the power flowing in the sensing medium, and p_{total} is the total power flowing in the whole waveguide. Noting that in a HCMW sensor, since h_1 is sub-millimeter scale, while $1/\alpha_2$ is wavelength scale, it is obvious that p_{guide}/p_{total} approaches to 1 without any question. As to another factor in Eq. (5), since n_{guide} is the refractive index of the guiding medium, and $N \to 0$ when ultrahigh-order modes are used as sensor's probe, therefore, $(n_{guide}/N) \gg 1$ is fulfilled in any case. It means that S_2 can easily be greater than 1.

In the evanescent field sensors, taking a reverse symmetrical waveguide (RSW) as an example, the analogous equations are cast in the form [13,27,28]

$$S_2 = \frac{\partial N}{\partial n_{cover}} = \frac{n_{cover}}{N} \cdot \frac{p_{cover}}{P_{total}}, \tag{7}$$

and

$$\frac{p_{cover}}{p_{total}} = \frac{\kappa_1^2}{\alpha_2(\kappa_1^2 + \alpha_2^2)(h_1 + 2/\alpha_2)}, \tag{8}$$

where n_{cover} and p_{cover} represent the refractive index and the power in the cover medium where the sensing analyte is located, respectively. Investigating Eq. (8), it is found that p_{cover}/p_{total} is hardly to attain the value of 1, even at the cut-off thicknesses of the guiding layer. Moreover, since N is always great than n_{cover} in the conventional optical waveguides or the surface plasmon structure. Consequently, $n_{cover}/N < 1$ and $S_2 < 1$ in turn are hold under any circumstance. Simulations for sensitivity and the compositions of four type biosensors are listed in Table 1 and Table 2 respectively. Theoretical analysis indicates that both S_1 and S_2 of the HCMW biosensor are considerably higher than that of the other

Table 1
Sensor's sensitivities for different optical biosensor: SPR, LRSPR, MCWG and HCMW.

Sensor types	FWHM	S_1	S_2	S_1
SPR	6.76	13	2.57	33
LRSPR	0.19	301	0.45	135
MCWG	0.52	189	0.92	174
HCMW	0.02	3675	6.01	22086

three biosensors. The integration improvement of the sensitivity and the detection limit by a few orders of magnitude are completely possible.

4. Experimental

4.1. Materials

In the sample fabrication, the required glucose injection was purchased from Hunan Zhongnan Kelun Pharmaceutical Co., Ltd, China. A set of glucose solution with concentrations change of 2 ppm (0.011 mmol/L) were obtained by calculating the ratios of glucose and de-ionized water in weight percentage. An 8-mm equilateral glass prism with a big vertex angle of 150° was coated with a thin gold film via DC sputtering to serve as the coupling layer. This allowed light incident on the prism at a small angle to excite the ultrahigh-order modes. A relative thicker gold film was sputtered on a polished glass chip to act as the substrate. A glass gasket of 5 mm in radius and about 0.7 mm in depth which was glued together with the substrate by using a UV-curable epoxy. The glass prism was then placed on the gasket to form a hollow cell to work as the sample room. With the help of a peristaltic pump, analyte solution to be detected flow into the cell through the inlet and the outlet tubes embedded in the substrate glass plate. Before the detection, a test experiment has been performed to precisely determine the parameters of the HCMW, and the result is given as follows: $h_1 = 688\,\mu m, \varepsilon_2 = -28 + 1.8i, n_3 = 1.503, h_2^{thin} = 38$ nm and $h_2^{thick} = 300$ nm. The incident wavelength is adjusted to be 860.00 nm. The thickness and the complex dielectric permittivity of the thin gold film are determined by the double-wavelength method [29] and the thickness of the guiding layer (hollow core) is determined by the m-line spectroscopy technique [24]. Since the thick gold film is used as the substrate, it is thick enough and its thickness is evaluated by the sputtering time.

4.2. Measurement

The schematic diagram of the experimental setup is shown in Fig. 5. To excite the ultrahigh-order mode of the HCMW, a TE polarized laser beam from a tunable laser (DL100, Topica Photonics) with a divergence angle of 0.4 mrad is induced to impinge upon the thin gold film of the HCMW biosensor which is located on a computer controlled $\theta/2\theta$ goniometer. Two apertures with a diameter of 1 mm and a distance of 0.5 m between them are inserted to further confine the divergence of the incident light. The reflected light is detected by a photodiode PD2. Another part of the beam, which comes from a beam splitter BS1, irradiates the second beam

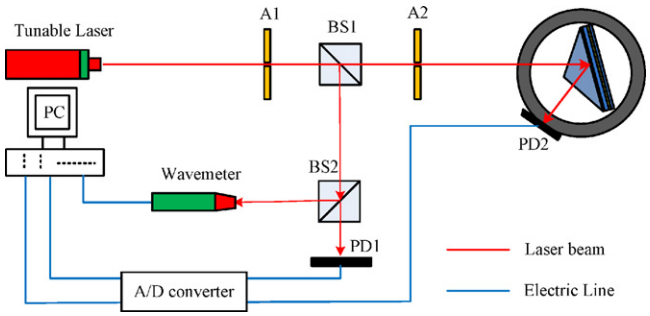

Fig. 5. Experimental set up of the HCMW biosensor.

splitter BS2 and splits into two beams. One is detected by PD1 as a reference in order to remove the intensity fluctuation. The remaining light is fed to a wavelength meter (COHERENT, Wavemaster) connected to a computer. In the experiment, the actual reflectivity is the product of the coupling ratio of PD2 to PD1 and the split ratio. In order to monitor the concentration variation of the analyte solution which is injected into the analyte room with the rate of 50 μL/s, a recoded ATR spectrum for one of the ultrahigh-order modes produced by angle scanning is shown in the inset of Fig. 6. It is demonstrated that a shift of the ATR spectrum occurs with the increasing of the analyte concentration of 10 ppm. In this angular exploration mode, the concentration change of the analyte solution is determined by detecting the position shift of the ATR dip. In order to further enhance the sensitivity, the HCMW biosensor is operated with intensity interrogation scheme. The incident angle is fixed near the midpoint of the falling edge of a selected dip. As the glucose concentration was changed subsequently from 0 to 2, 4, 6 and 8 ppm in the steps, the operation position moves from the midpoint to the upside of the probing curve, which results in the increases of the reflectivity.

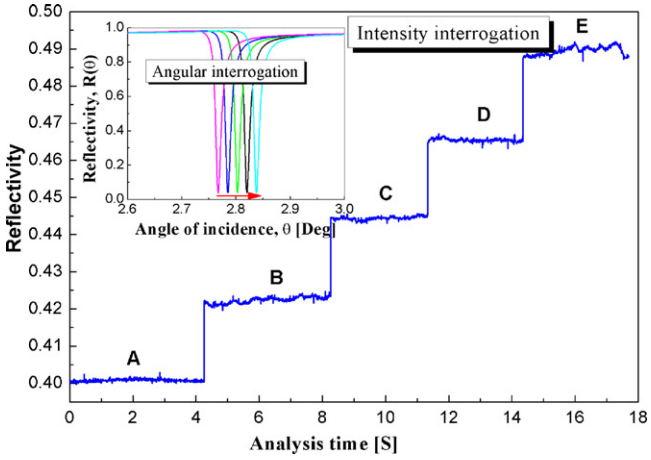

Fig. 6. Changes of reflectivity with variation of glucose concentration. (a) deionized water, (b) 2 ppm glucose solution, (c) 4 ppm glucose solution, (d) 6 ppm glucose solution, and (e) 8 ppm glucose solution. Insert is angular interrogation in which the glucose concentration is increasing with 10 ppm.

Table 2
Parameters chosen for the four biosensor types being studied [10,16,27].

Sensor	HCMW	SPR	LRSPR	MCWG
Polarization	TE	TM	TM	TE
Prism (n_3)	1.517	1.517	1.517	1.517
Buffer (n_b, h_b)	–	–	1.333 887 nm	–
Metal (ε_2, h_2)	−10.2 + i1.0, 50 nm	−16.0 + i0.52, 56 nm	−10.2 + i1.0, 15.2 nm	−16.0 + i0.52, 60 nm
Guiding (n_1, h_1)	1.330, 700 μm	–	–	1.59, 330 nm
Substrate (ε_s or n_s)	−10.2 + i1.0	1.330	1.330	1.330

5. Discussion

Fig. 6 illustrates the performance of the HCMW device when used with low concentrations of glucose. The step-style change of concentrations is 2 ppm, with the average 2.3% change in the reflectivity. According to noise level [30–32] and the assumption that the photodiode detection limit of the reflected light is 0.5%, the new biosensor has been shown to be capable of directly detecting concentration of glucose as low as 0.5 ppm, which corresponds to a high resolution of 1.4×10^{-7} RI units [22]. The reason for the obtained relative high sensitivity maybe that our detect probe is the oscillating field (see Fig. 1(c)) not the evanescent field. The sensitivity of biosensor is closely related to the ratio of light energy interacted with the analyte, the bigger ratio, the higher sensitivity [4]. The ratio of energy of evanescent field is far less than that of the oscillating field, thus the performance of the oscillating field is better. The strong confinement of the light power in the guiding region could result in a sufficient interaction between light and the analyte solution. Owing to the sensor's high sensitivity, the temperature variation of the system becomes one of the major noise sources. In our experiment, the room-temperature is held constant at 22.4 °C and is monitored by a thermal couple. Morever, both the biosensor and the samples are placed in a thermal shield box made of the polymethyl methacrylate. Temperature change in the thermal shield box is constant to about 0.1 °C in a short time duration. Since the temperature coefficient of the refractive index of water sample between 20 and 30 °C, on average [33], is 1.0×10^{-4} °C^{-1}, the repeatable experiment result demonstrates that variation of temperature in the thermal shield box is less than 0.01 °C within several minutes detection.

Another important parameter of an HCMW biosensor is its operating range. It is noted that the zone of linearity with intensity interrogation scheme is limited, and this mode is suit for the measurement of extremely lower concentration. In the case of a relative higher concentration, an angular interrogation scheme is recommended, which exhibits a large linear region of detection.

6. Conclusion

In conclusion, a novel biosensor based on a hollow core metal cladding waveguide has been proposed and characterized. The measurements performed have shown that a refractive-index change of 1.4×10^{-7} can be unambiguously identified. This study has also revealed that strong confinement of the light power in the guiding region results in a sufficient interaction between light and the analyte solution, which makes the response time greatly reduced. Aside from higher detection efficiency, the proposed biosensor platform is simple to fabricate by conventional technology and enables label-free and real-time detection.

Acknowledgements

This research was supported by the National Natural Science Foundation of China (Nos. 10874121, 10874119, 10474093 and 61168002) and the National Basic Research Program "973" of China (Contract No. 2007CB307000), and the Foundation for Development of Science and Technology of Shanghai (Grant No. 10JC1407200), and the opening foundation by state key laboratory of advanced optical communication systems and networks, Shanghai Jiaotong University of China (No. 2011GZKF031105).

References

[1] C. McDonagh, C.S. Burke, B.D. MacCraith, Optical chemical sensors, Chemical Reviews 108 (2008) 400–422.
[2] J. Wang, Electrochemical glucose biosensors, Chemical Reviews 108 (2008) 814–825.
[3] Y. Lin, F. Lu, Y. Tu, Z. Ren, Glucose biosensor based on carbon nanotube nanoelectrode ensembles, Nano Letters 4 (2004) 191–195.
[4] X. Fan, I.M. White, S.I. Shopova, H. Zhu, J.D. Suter, Y. Sun, Sensitive optical biosensor for unlabeled targets: a review, Analytica Chimica Acta 620 (2008) 8–26.
[5] M.J. Levene, J. Korlach, S.W. Turner, M. Foquet, H.G. Craighead, W.W. Web, Zero-mode waveguides for single-molecule analysis at high concentrations, Science 299 (2003) 682–686.
[6] F. Vollmer, S. Arnold, Whispering-gallery-mode biosensing: laber-free detection down to single molecules, Nature Methods 5 (2008) 591–596.
[7] D.J. Bornhop, J.C. Latham, A. Kussrow, D.A. Markov, R.D. Jones, H.S. Sorensen, Free-solution label-free molecular interactions studied by back-scattering interfometry, Science 317 (2007) 1732–1736.
[8] J. Homola, Surface plasmon resonance sensors for detection of chemical and biological species, Chemical Reviews 108 (2008) 462–493.
[9] X.D. Hoa, A.G. Kirk, M. Tabrizian, Towards integrated and sensitive surface plasmon resonance biosensors: a review of recent progress, Biosensors and Bioelectronics 23 (2007) 151–160.
[10] C.J. Huang, J. Dostalek, A. Sessitsch, W. Knoll, Long-range surface plasmon-enhanced fluorescence spectroscopy biosensor for ultrasensitive detection of *E. coli* O157:H7, Analytical Chemistry 83 (2011) 674–677.
[11] H.J. Watts, C.R. Lowe, Optical biosensor for monitoring microbial cells, Analytical Chemistry 66 (1994) 2465–2470.
[12] M. Zourob, S. Mohr, B.J.T. Brown, P.R. Fielden, M.B. McDonnellc, N.J. Goddard, Bacteria detection using disposable optical leaky waveguide sensors, Biosensors and Bioelectronics 21 (2005) 293–302.
[13] R. Horvath, H.C. Pedersen, Demonstration of reverse symmetry waveguide sensing in aqueous solutions., Applied Physics Letters 81 (2002) 2166–2168.
[14] M. Zourob, S. Mohr, B.J.T. Brown, P.R. Fielden, M.B. McDonnellc, N.J. Goddard, An integrated optical leaky waveguide sensor with electrically induced concentration system for the detection of bacteria, Lab Chip 5 (2005) 1360–1365.
[15] M. Zourob, S. Mohr, B.J.T. Brown, P.R. Fielden, M.B. McDonnellc, N.J. Goddard, An integrated metal clad leaky waveguide sensor for detection of bacteria, Analytical Chemistry 77 (2005) 232–242.
[16] N. Skivesen, R. Horvath, S. Thinggaard, N.B. Larsen, H.C. Pedersen, Deep-probe metal-clad waveguide biosensor, Biosensors and Bioelectronics 22 (2007) 1282–1288.
[17] G. Rong, A. Najmaie, J.E. Sipe, S.M. Weiss, Nanoscale porous silicon waveguide for label-free DNA sensing, Biosensors and Bioelectronics 23 (2008) 1572–1576.
[18] T. Dallas, P.K. Dasgupta, Light at the end of the tunnel: recent analytical applications of liquid-core waveguides, Trends in Analytical Chemistry 23 (2004) 1–8.
[19] I.P. Kaminow, W.L. Mammel, H.P. Weber, Metal-clad optical waveguides: analytical and experimental study, Applied Optics 13 (1974) 396–405.
[20] H. Li, Z. Cao, H. Lu, Q. Shen, Free-space coupling of a light beam into a symmetrical metal-cladding optical waveguide, Applied Physics Letters 83 (2003) 2757–2759.
[21] H. Lu, Z. Cao, H. Li, Q. Shen, Study of ultrahigh-order modes in a symmetrical metal-cladding optical waveguide, Applied Physics Letters 85 (2004) 4579–4581.
[22] W.W. Lam, L.H. Chu, C.L. Wong, Y.T. Zhang, A surface plasmon resonance system for the measurement of glucose in aqueous solution, Sensors and Actuators B 105 (2005) 138–143.
[23] H.V. Hsieh, Z.A. Pfeiffer, T.J. Amiss, D.B. Sherman, J.B. Pitner, Direct detection of glucose by surface plasmon resonance with bacterial glucose/galactose-binding protein, Biosensors and Bioelectronics 19 (2004) 653–660.
[24] P.K. Tien, R. Ulrich, R.J. Martin, Modes of propagating light waves in thin deposited semiconductor films, Applied Physics Letters 14 (1969) 291–294.
[25] A.A. Kolomenskii, P.D. Gershon, H.A. Schuessler, Sensitivity and detection limit of concentration and absorption measurements by laser-induced surface-plasmon resonance, Applied Optics 36 (1997) 6539–6547.
[26] H. Tiefenthaler, W. Lukosz, Sensitivity of grating couplers as integrated-optical chemical sensors, Journal of the Optical Society of America B: Optical Physics 6 (1989) 209–220.
[27] F.C. Chien, S.J. Chenb, A sensitivity comparison of optical biosensors based on four different surface plasmon resonance, Biosensors and Bioelectronics 20 (2004) 633–642.
[28] K. Tiefenthaler, W. Lukosz, Sensitivity of grating couplers as integrated-optical chemical sensors, Journal of the Optical Society of America B: Optical Physics 6 (1989) 209–220.
[29] W.P. Chen, J.M. Chen, Use of surface plasma waves for determination of the thickness and optical constants of thin metallic films, Journal of The Optical Society of America B: Optical Physics 71 (1981) 189–191.
[30] B. Ran, S.G. Lipson, Comparison between sensitivities of phase and intensity detection in surface plasmon resonance, Optics Express 14 (2006) 5641–5650.
[31] M. Piliarik, J. Homola, Surface plasmon resonance (SPR) sensors: approaching their limits, Optics Express 17 (2009) 16505–16517.
[32] A.V. Kabashin, S. Patskovsky, A.N. Grigorenko, Phase and amplitude sensitivities in surface plasmon resonance bio and chemical sensing, Optics Express 17 (2009) 21191–21204.
[33] R.C. Weast, CRC Handbook of Chemistry and Physics, 68th ed., CRC Press, Boca Raton, F.L, 1978.

Biographies

Pingping Xiao, born in 1972, is currently a PhD candidate in Department of Physics, Shanghai JiaoTong University, China. He received his master degree on optics from Jiangxi Normal University, China, in 2004. He is currently an associate professor in Department of Physics, Yuchun University, China. His research interests include application of optical waveguide and bio-chemical biosensor.

Xianping Wang, born in 1984, is currently a PhD candidate in Department of Physics, Shanghai JiaoTong University, China. He received his master degree on optics from Jiangxi Normal University, China, in 2010. His research interests include application of optical waveguide, Goos-Hänchen shift and optical bistability.

Jingjing Sun, born in 1986, is currently a PhD candidate in Department of Physics, Shanghai JiaoTong University, China. She received her master degree on optics from Jiangxi Normal University, China, in 2009. Her research interests include bio-chemical sensor and magnetical fluid.

Honggen Li, born in 1979, he received the PhD degree in applied physics from Department of Physics, Shanghai JiaoTong University, China, in 2006. He is currently an associate professor in Department of Physics, Shanghai JiaoTong University, China. His research interests include optical waveguide design and electro-optical devices design.

Meizhen Huang, born in 1966, she received the PhD degree in optical engineering from Department of Physics, Zhejiang University, China, in 2001. She is currently a professor and PhD candidate supervisor in Department of Physics, Shanghai Jiao-Tong University, China. Her research interests include spectral analysis and position sensitive device design.

Xianfeng Chen, born in 1967, he received the PhD degree in optics from Department of Physics, Shanghai JiaoTong University, China, in 1995. He is currently a professor and PhD candidate supervisor in Department of Physics, Shanghai JiaoTong University, China. His research interestes include nonliner optics and magnetical fluid.

Zhuangqi Cao, born in 1945, he received the Master degree in optics from Department of Physics, Shanghai JiaoTong University, China, in 1982. He is currently a professor and PhD candidate supervisor in Department of Physics, Shanghai JiaoTong University, China. His research interests include application of optical waveguide, Goos-Hänchen shift and bio-chemical sensor.